ChemComm

Accepted Manuscript

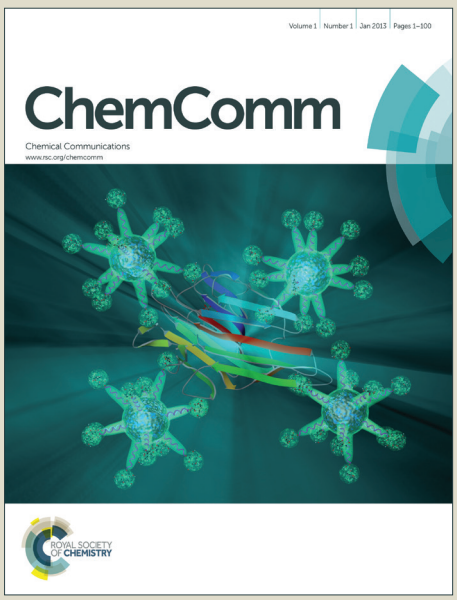

ROYAL SOCIETY OF CHEMISTRY

www.rsc.org/chemcomm

ARTICLE TYPE www.rsc.org/xxxxxx | XXXXXXXX

Redox-Triggered Changes in the Self-Assembly of a Ferrocene-Peptide Conjugate

Bimalendu Adhikari and Heinz-Bernhard Kraatz*

Received (in XXX, XXX) Xth XXXXXXXXX 200X, Accepted Xth XXXXXXXXX 200X
DOI: 10.1039/b000000x

Ultrasonication of a ferrocene conjugate of a short amyloid peptide (Aβ18–20) in toluene causes formation of an organogel, which undergoes dramatic structural changes upon oxidation from a nanofibrillar network to spherical micelles. This morphological change is redox-controlled and reversible.

The self-assembly of small molecules has attracted increasing interest to construct functional soft materials. The use of low-molecular-weight gels that, undergo reversible dissociation and association by non-covalent interactions, is attractive due to the dynamic nature of these systems and their versatility.[1] In this context, the stimuli-responsiveness is of particular interest and plays a crucial role in functional soft materials.[2] Light,[3] sound,[4] pH,[5] solvent,[6] temperature,[1] ions,[7] enzymes,[8] and others[9] are frequently used as stimuli to alter the behavior of the molecular assembly for functional expression. Redox-trigerred self-assembly of supramolecular systems is much less common.[10] The construction of redox-active soft materials that efficiently produce redox-induced morphological transformations is an attractive goal in the design of functional stimuli-responsive materials.

Ferrocene (Fc)-peptide conjugates have received significant attention for their interesting structural properties and their potential bioanalytical applications.[11,12,13] Organogels and hydrogels of Fc-peptides are not common.[14] Recently, the simple conjugate FcCO-Phe-OH has been reported to form a hydrogel.[14a] In our own work, we have demonstrated the use of some Fc-peptide conjugates to form organogels.[14b] Here, we report a supramolecular transformation of FcCO-Val-Phe-Phe-OMe (**1**) from a nanofibrous gel to a spherical micelle, where the peptide fragment of the conjugate corresponds to the hydrophobic amyloid sequence Aβ18–20 (see Scheme 1).

FcCO-Val-Phe-Phe-OMe (Fc-peptide **1**) is readily soluble in toluene with increasing temperature. TEM studies reveal the formation of a nanorod morphology for the assembled conjugate **1** at room temperature (*vide infra*). Upon cooling of a hot solution to room temperature followed by ultrasonication, a gel phase material is obtained. The minimum gelation concentration is 1.4%, w/v with a gel melting temperature of 56°C. Rheological experiments confirm G′>G″ (Fig. S1; ESI). It is important to note that in the absence of ultrasound, no gel is obtained. After ultrasonication, a cross-linked nanofibrillar morphologies is observed, indicating that sonication is critical for this change in morphology from nanorods to networks of cross-linked nanofibers. It can be rationalized that ultrasound could assist faster intermolecular hydrogen bond formation and may induce structural changes of the Fc-peptide **1** that facilitates formation of interconnected nanofibers and hence gelation.

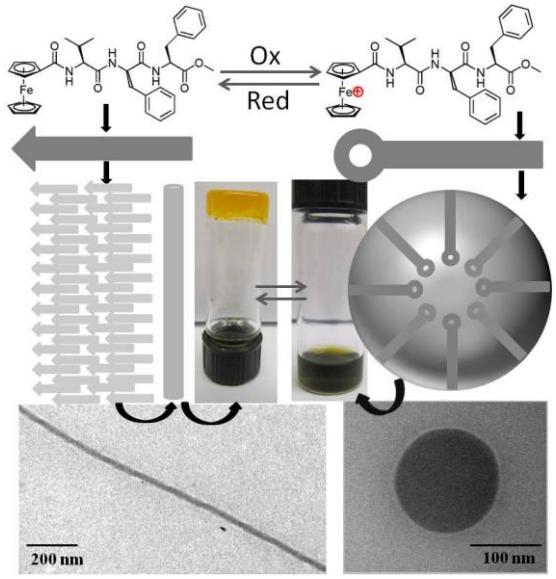

Scheme 1. Schematic representation for redox induced morphological transformations of Fc-peptide **1** by different mode of assembly. Fc-peptide **1** self-assemble into β-sheet like conformation to form nanofibrous gel, which upon oxidation produces micelle-like spherical structure. TEM images of a single fiber and micellar spheroid are shown (below).

Importantly, the reverse sequence peptide FcCO-Phe-Phe-Val-OMe (Fc-peptide **2**) and other structurally similar tripeptides including FcCO-Ala-Phe-Phe-OMe (Fc-peptide **3**), FcCO-Leu-Phe-Phe-OMe (Fc-peptide **4**), having non-amyloidogenic sequences, do not form gels even at higher concentration and application of ultrasound. TEM studies also demonstrate that these non-amyloidogenic peptides do not form any ordered nanofibrillar cross-linked structures (Fig. S2; ESI). This suggests that amyloidgenic sequence in Fc-peptide **1** is responsible for gelation, presumably through β-sheet formation. This assumption is supported by FT-IR studies of gels that exhibit a band at 1622 cm^{-1}, characteristic of β-sheet structures (Fig. S3; ESI). FTIR studies also suggest significant differences in peak positions between gelator Fc-peptide **1** and non-amyloidogenic Fc-peptides **2-4** (Fig. S4; ESI). An XRD study of Fc-peptide **1** exhibits a sharp signal with d-spacing of 5.04 Å (spacing between peptide chains) accompanied by another signal at 11.72 Å, which is characteristic of spacing between β-sheet layers,[15] suggesting the presence of a β-sheet structure in the gel state (Fig. S5; ESI).

Solvent and temperature dependent ^{1}H-NMR studies were performed to investigate the molecular interactions in the self-

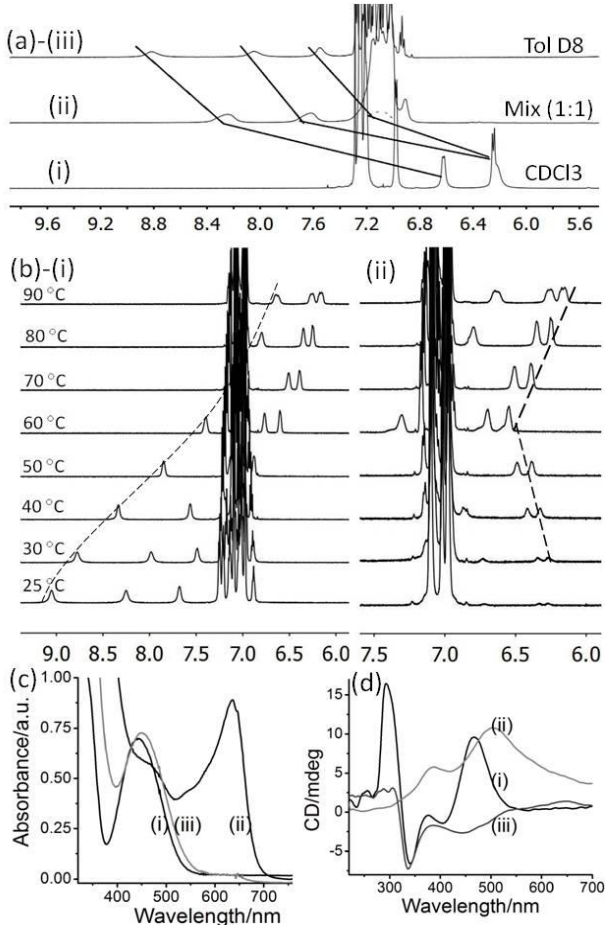

Fig. 1 Spectroscopic behaviour of Fc-peptide **1**. (a) Solvent titration ^{1}H-NMR study of Fc-peptide **1** at room temperature as a function solvent composition (in $CDCl_3$-TolueneD_8): (i) 100% $CDCl_3$ (ii) 50% $CDCl_3$-50% TolueneD_8 (iii) 100% TolueneD_8. (b) VT-NMR in Tolene D8: (i) a solution with out treatment of ultrasound, on cooling starting from 90 °C (ii) ultrasound induced a gel phase material, on heating starting from 25 °C. (c) UV-Vis studies of Fc-peptide **1**: (i) before oxidation, (ii) after oxidation and (iii) reduction of ii. (d) CD studies of Fc-peptide **1**: (i) sol state with out treatment of ultrasound (ii) gel state after treatment of ultrasound and (c) oxidized state.

assembled state (Fig. 1a,b). Solvent titration NMR spectroscopic studies were carried out as a function of solvent composition (in a mixture of $CDCl_3$-toluene-D_8, as chloroform is a non-gelling solvent). A downfield shift (1.3-2.2) of all amide protons is observed in toluene-D_8 compared to $CDCl_3$, suggesting strong intermolecular H-bonding interactions in toluene, which serves as the gelling solvent. To confirm that changes in chemical shifts are caused by intermolecular interaction rather than solvation effects, VT-NMR spectroscopic experiments were carried out with a solution of the Fc-peptide **1** in toluene-D_8 (see ESI for a full charcaterization by gCOSY, gHMBCAD). With a gradual decrease in temperature, the amide protons of Val(1), Phe(3) and Phe(2) shift downfield and at 25 °C give rise to signals at 7.66, 8.22 and 9.01 ppm, respectively (Fig. 1b(i) and Fig. S6, ESI). The temperature coefficient of the amide protons are 29.9 ppb K^{-1} for Val(1), 46.6 ppb K^{-1} for Phe(2) and 41.5 ppb K^{-1} for Phe(3) (Fig. S6; ESI for detail). These values are significantly higher than that of other H-bonded Fc-peptides previously reported,[13] suggesting the formation of very strong intermolecular hydrogen bonding interactions. Upon heating the ultasound-induced gel-phase material all amide protons gradually shift downfield, up to the gel melting temperature of 60 ºC. (Fig. 1b(ii) and Fig. S7; ESI). After gel melting, the amide protons shift upfield (up to the observation maximum of 90 °C), which may be rationalized by considering a temperature dependent equilibrium between aggregated and non-aggregated gelators. (see Fig. S7, ESI for a more detailed explanation).

The gel is thermo-reversible; it melts upon heating and reverses into a gel upon cooling and sonication. We examined the effect of oxidation on the assembly behavior of a gel of Fc-peptide **1**. Treating the organogel with an equimolar amount of the oxidizing agent $Fe(ClO_4)_3$, a gradual degradation of the gel is observed resulting in a non-gel state within minutes. The transformation is accompanied by a distinct colour change from light orange to deep blue (Scheme 1). This colour change is due to the oxidation of ferrocene (Fc) to ferrocenium (Fc^+). To probe the reversible redox behavior of Fc-peptide **1**, UV-Vis spectroscopic experiments were performed in acetone (Fig. 1c). Fc-peptide **1** gives rise to an absorbance at λ = 446 nm. Upon addition of the oxidant, the signal at 446 nm decreases and a signal due to the formation of the Fc^+ state is observed at λ = 636 nm. The signal at 446 nm reappeared after reduction of ferrocenium moiety by ascorbic acid, suggesting that this oxidation and reduction process is completely reversible. Cyclic voltammetry (CV) of Fc-peptide **1** also showed reversible behavior with a halfwave potential of 455 mV (Fig. S8; ESI).

Circular dichroism (CD) studies of a solution of Fc-peptide **1** in toluene (without treatment of ultrasound) exibits an induced positive CD signal for ferrocene at 465 nm. Monosubstituted Fc-peptides generally do not exhibit a significant CD signal in the Fc region, since they generally do not induce axial chirality around the Fc core.[11] However, we can only speculate that self-assembly gives rise to this behaviour, resulting in a P-helical arrangement. Significantly, the Fc-based CD signal shifts to 504 nm for the ultrasound-induced gel state (Fig. 1d), indicating that formation of the gel causes conformational changes in the Fc-peptide, while maintaining the helicity of the Fc core. Upon oxidation of the gel, the Fc-based signal is lost and we speculate that this chiroptical change is again due to a structural reorganization of the Fc-peptide molecules.

To investigate the morphological features of the self-assembling Fc-peptide **1**, TEM studies were performed before and after sonication. Before sonication, the Fc-peptide **1** exclusively possesses a nanorod-like morphology with an average diameter of 170 nm and a length of a few micrometers (Fig. 2a). In contrast, the TEM of the ultrasound induced gel phase material indicates the formation of a uniform, well-ordered cross-linked nanofibrillar network structure (Fig. 2b). These fibrils have a high aspect ratio, with an average width of 45 nm and a length of a few micrometers.

Upon oxidation of the gel, the fibrillar structure is lost as is demonstrated in Fig. 2c and 2d. Partial oxidation of the gel

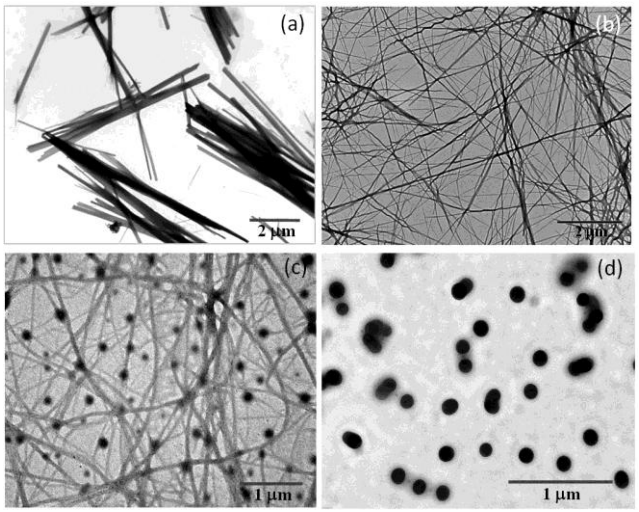

Fig. 2 TEM images of self-assembled Fc-peptide **1**: (a) with out (b) with treatment of ultrasound; (c) partially and (d) fully oxidized Fc-peptide **1** with $Fe(ClO_4)_3$.

gives rise to a mixture of nanofibers and objects having micellar, spherical morphologies. Stiochiometric oxidation of the gel results in the exclusive formation of spheres with an average diameter of 155 nm (Fig. 2c,d and Fig. S9). This compares favourably with the result obtained from dynamic light scattering study, which shows an average size of 158 nm (Fig. S10; ESI). Interestingly, this change in morphology is reversible and reduction of the spherical micelles with ascorbic acid, followed by sonication, results in the formation of fibrillar morphologies. Oxidation of the Fc-peptide gives rise to an ionic Fc^+-head group that together with ClO_4^- counter ions, will assemble to form the inside of the micelle with the hydrophobic peptides facing outwards in solution in order to maximize ionic interactions. (Scheme 1). Other examples of structural rearrangements of this type have been reported by Manners et al for unrelated ferrocenyl block copoymers.[10b] In the present study, the oxidation of the Fc group results in the formation of micelle-like structures by the disruption of the ordered β-sheet structure of the Aβ18–20 peptide, which is evident by FT-IR and XRD studies (Fig. S3 and Fig. S5; ESI). FT-IR studies of oxidized Fc-peptide **1** exhibit complete loss of the band at 1622 cm^{-1}, suggesting disruption of β-sheet structure in the oxidised state (Fig. S3; ESI).

In conclusion, the results demonstrate that the Fc-conjugate of Aβ18–20 engages in intermolecular H-bonding, giving rise to an induced Fc-based CD signal and it forms an organogel upon ultrasonication. In addition, the Fc-peptide shows ultrasound induced morphological trasformation from nanorod to nanofiber. Interestingly, the organogel undergoes dramatic redox triggered structural changes from a fibrillar network to micelles. This presumably results from solvation effects, where micelle formation is driven by minimizing the interaction of the ionic Fc^+ group with the hydrophobic solvent toluene, which effectively solubilizes the peptide component of the bioorganometallic conjugate. There is evidence that this structural rearrangement results from loss of the β-sheet interactions between adjacent peptide segments. This study demonstrates that redox, as a stimulus, may serve as a versatile tool to control the self-assembly of peptides, which may enable us to develop new redox-active functional biomaterials in the near future.

Notes and references

* *Department of Physical and Environmental Sciences, University of Toronto Scarborough, 1265 Military Trail, Toronto, M1C 1A4, Canada and Department of Chemistry, University of Toronto, 80 St. George Street, Toronto, Ontario M5S 3H6, Canada.*
E-mail: bernie.kraatz@utoronto.ca

† Electronic Supplementary Information (ESI) available.

1 (a) A. R. Hirst, B. Escuder, J. F. Miravet and D. K. Smith, *Angew. Chem. Int. Ed.*, 2008, **47**, 8002 – 8018. (b) C. Yan and D. J. Pochan, *Chem. Soc. Rev.*, 2010, **39**, 3528–3540. (c) S. Banerjee, R. K. Das and U. Maitra, *J. Mater. Chem.*, 2009, **19**, 6649–6687. (d) M.-O. M. Piepenbrock, G. O. Lloyd, N. Clarke and J. W. Steed, *Chem. Rev.*, 2010, **110**, 1960–2004. (e) A. Dawn, T. Shiraki, S. Haraguchi, S.-i.Tamaru and S. Shinkai, *Chem. Asian J.* 2011, **6**, 266 – 282.

2 G. R. Whittell, M. D. Hager, U. S. Schubert, I. Manners, *Nat. Mater.*, 2011, **10**, 176–188.

3 (a) Z. Qiu, H. Yu, J. Li, Y. Wang and Y. Zhang, *Chem. Commun.* **2009**, 3342–3344. (b) C. Wang, Q. Chen, F. Sun, D. Zhang, G. Zhang, Y. Huang, R. Zhao and D. Zhu, *J. Am. Chem. Soc.*, 2010, **132**, 3092–3096.

4 (a) K. Isozaki, H. Takaya and T. Naota, *Angew. Chem. Int. Ed*. 2007, **46**, 2855 –2857. (b) X. Yu, Q. Liu, J. Wu, M. Zhang, X. Cao, S. Zhang, Q. Wang, L. Chen and T. Yi, *Chem.–Eur. J.*, 2010, **16**, 9099. (c) S. Maity, P. Kumar and D. Haldar, *Soft Matter*, 2011,**7**, 5239-5245.

5 D. J. Adams and P. D. Topham, *Soft Matter*, 2010, **6**, 3707–3721.

6 Q. Jin, L. Zhang and M. Liu, *Chem. Eur. J.*, 2013, **19**, 9234 – 9241.

7 (a) A. Ajayaghosh, P. Chithra, R. Varghese and K. P. Divya, *Chem. Commun.*, 2008, 969 – 971. (b) H.-J. Kim, J.-H. Lee and M. Lee, *Angew. Chem. Int. Ed.*, 2005, **44**, 5810 – 5814.

8 (a) Y. Gao, F. Zhao, Q. Wang, Y. Zhang and B. Xu, *Chem. Soc. Rev.*, 2010, **39**, 3425–3433. (b) J. W. Sadownik, J. Leckie and R. V. Ulijn, *Chem. Commun.*, 2011, **47**, 728–730.

9 W. Cao, X. Zhang, X. Miao, Z. Yang and H. Xu, *Angew. Chem. Int. Ed.*, 2013, **52**, 1 – 6.

10 (a) M. Nakahata, Y. Takashima, H. Yamaguchi and A. Harada, *Nat. Commun.*, 2011, **2**, 511. (b) J.-C. Eloi, D. A. Rider, G. Cambridge, G. R. Whittell, M. A. Winnik and I. Manners, *J. Am. Chem. Soc.*, 2011, **133**, 8903–8913. (c) J. Liu, P. He, J. Yan, X. Fang, J. Peng, K. Liu and Y. Fang, *Adv. Mater.*, 2008, **20**, 2508–2511. (d) Y. Zhang, B. Zhang, Y. Kuang, Y. Gao, J. Shi, X. X. Zhang, B. Xu, *J. Am. Chem. Soc.*, 2013, **135**, 5008–5011. (e) X. Sui, X. Feng, M. A. Hempenius and G. J. Vancso, *J. Mater. Chem. B*, 2013, **1**, 1658–1672. (f) B. Adhikari, R. Afrasiabi and H.-B. Kraatz, *Organometallics* 2013, **32**, 5899−5905.

11 (a) D. R. van Staveren and N. Metzler-Nolte, *Chem. Rev.*, 2004, **104**, 5931–5985. (b) T. Moriuchi and T. Hirao, *Acc. Chem. Res.* **2010**, *43*, 1040–1051.

12 S. Martić, M. Labib, P. O. Shipman and H.-B. Kraatz, *Dalton Trans.*, **2011**, *40*, 7264–7290.

13 S. Beheshti, S.Martić and H.-B. Kraatz, *Chem. Eur. J.*, 2012, **18**, 9099–9105.

14 (a) Z. Sun, Z. Li, Y. He, R. Shen, L. Deng, M. Yang, Y. Liang and Y.Zhang, *J. Am. Chem. Soc.*, 2013, **135**, 13379−13386. (b) R. Afrasiabi and H.-B. Kraatz, *Chem. Eur. J.*, 2013, **19**, 17296 – 17300.

15 G. Palui, J. Nanda, S. Ray and A. Banerjee, *Chem. Eur. J.*, 2009, **15**, 6902 – 6909.